HHS Public Access

Author manuscript

Sci Bull (Beijing). Author manuscript; available in PMC 2021 December 08.

Published in final edited form as:

Sci Bull (Beijing). 2020 August 15; 65(15): 1281–1296. doi:10.1016/j.scib.2020.03.040.

Reprogramming of Ovarian Granulosa Cells by YAP1 Leads to Development of High-Grade Cancer with Mesenchymal Lineage and Serous Features

Xiangmin Lv[1,2,12], **Chunbo He**[2,3,12], **Cong Huang**[1], **Guohua Hua**[1,3], **Xingcheng Chen**[4,5], **Barbara K. Timm**[6], **Victoria M Maclin**[6], **Abigail A Haggerty**[7], **Shelly K Aust**[7], **Denae M Golden**[7], **Bhavana J Dave**[7], **Yun-An Tseng**[5], **Li Chen**[1,8], **Hongbo Wang**[1], **Peichao Chen**[1,9], **David L Klinkebiel**[10], **Adam R Karpf**[4], **Jixin Dong**[4], **Ronny I Drapkin**[11], **Bo R Rueda**[1], **John S Davis**[2,4], **Cheng Wang**[1,2]

[1]Vincent Center for Reproductive Biology, Department of Obstetrics and Gynecology, Massachusetts General Hospital, Harvard Medical School, Boston, MA 02114, USA.

[2]Olson Center for Women's Health, Department of Obstetrics and Gynecology, University of Nebraska Medical Center, Omaha, NE 68198, USA.

[3]College of Animal Sciences and Veterinary Medicine, Huazhong Agricultural University, Wuhan 47000, China;

[4]Fred & Pamela Buffett Cancer Center, University of Nebraska Medical Center, Omaha, NE 68198, USA.

[5]Department of Pathology and Microbiology, University of Nebraska Medical Center, Omaha, NE 68198, USA.

[6]Heartland Center for Reproductive Medicine, Omaha, NE 68198, USA.

[7]Munroe-Meyer Institute, University of Nebraska Medical Center, Omaha, NE 68198, USA.

[8]Key Laboratory of Animal Ecology and Conservation Biology, Institute of Zoology, Chinese Academy of Sciences, Beijing 100101, China

[9]College of Life and Environmental Science, Wenzhou University, Wenzhou 325035, China

[10]Biochemistry and Molecular Biology, University of Nebraska Medical Center, Omaha, NE 68198, USA.

[11]Department of Obstetrics and Gynecology, University of Pennsylvania, Philadelphia, PA 19104, USA.

Corresponding Author: Cheng Wang, Ph.D., Investigator, Department of Obstetrics and Gynecology, Massachusetts General Hospital, Associate Professor, Harvard Medical School, Boston, MA 02114, Phone: 617-624-1616, cwang34@mgh.harvard.edu.

AUTHOR CONTRIBUTIONS

Lv X and He C contributed to the experimental design, performance, data analysis, and manuscript preparation. Hua G, Huang C, Chen X, Dong J, Chen L, Wang H, and Chen P assisted in completing *in vivo* experiments and data analysis. Timm BK and Maclin VM assist in the preparation of primary cells. Haggerty AA, Aust SK, Golden DM, and Dave BJ performed aCGH analysis. Karpf AR and Klinkebiel DL conducted the DNA methylation analysis. Tseng Y and Drapkin RI assisted in the pathological analysis. Davis JS contributed to the data analysis and manuscript preparation. Rueda B contributed to manuscript editing. Wang C supervised these studies and contributed to the experimental design, data analysis, and manuscript preparation.

[12]Equal contributors

Disclosures: The authors have no competing interests to declare

Abstract

Understanding the cell-of-origin of ovarian high grade serous cancer (HGSC) is the prerequisite for efficient prevention and early diagnosis of this most lethal gynecological cancer. Recently, a mesenchymal type of ovarian HGSC with the poorest prognosis among ovarian cancers was identified by both TCGA and AOCS studies. The cell-of-origin of this subtype of ovarian cancer is unknown. While pursuing studies to understand the role of the Hippo pathway in ovarian granulosa cell physiology and pathology, we unexpectedly found that the Yes-associated protein 1 (YAP1), the major effector of the Hippo signaling pathway, induced dedifferentiation and reprogramming of the ovarian granulosa cells, a unique type of ovarian follicular cells with mesenchymal lineage and high plasticity, leading to the development of high grade ovarian cancer with serous features. Our research results unveil a potential cell-of-origin for a subtype of HGSC with mesenchymal features.

Keywords

Ovarian granulosa cells; cell reprogramming; cell dedifferentiation; the Hippo pathway; YAP1 oncogene; Mesenchymal type of high grade serous cancer

INTRODUCTION

Ovarian cancer is the fifth leading cause of cancer death in women and the most lethal gynecological malignancy in the United States. Approximately 225,500 women are diagnosed with ovarian cancer annually, with an estimated 140,200 associated deaths worldwide [1]. The majority (~80%) of ovarian cancers have an epithelial origin and are subdivided into low-grade and high-grade serous carcinomas (HGSCs) [2, 3]. Low-grade serous carcinomas (LGSCs) make up a small percentage of the epithelial tumors and often exhibit multiple genetic mutations (e.g., KRAS, BRAF, ERBB2, *etc.*), low-grade nuclei (lacking nuclear atypia) with infrequent mitotic figures, and overall, patients have a better outcome as opposed to high-grade [2]. Ovarian HGSC constitutes 60%–80% of ovarian epithelial carcinomas and stands out from other subtypes of ovarian cancer because of their aggressive nature and unique genetic alterations (high rate *TP53* mutation, frequent *BRCA1/2* inactivation, and very common oncogene amplification) [4, 5]. HGSC is most frequently present at advanced clinical stages and patients have a very poor overall survival.

The site and cell of origin of ovarian HGSC are not fully understood. More often than not by the time the disease has been detected, the cancer cells are already widely spread to other tissues or organs, making it challenging to assess origin [6]. This could be attributed to the difficulties in identifying precursor lesions and the lack of biomarkers for preventive screening and timely detection. Early studies suggested that HGSC may be derived from the neoplastic transformation of ovarian surface epithelial (OSE) cells or ovarian cortical inclusion cyst epithelial cells [6]. However, recent evidence suggests that OSE cells or cells from the inclusion cysts may be the cell-of-origin of the LGSCs [2]. It is now accepted that a significant number of ovarian HGSC originate from the secretory epithelial cells in the fimbriae of fallopian tubes [6–13]. Interestingly, there is also evidence supporting the concept that LGSC could progress to HGSC [14–18].

The next-generation sequencing technology made it possible for scientists to classify ovarian HGSC based on their genomic signatures. By mining TCGA database and analyzing the gene expression profiles of ovarian high-grade serous cancer patients, the TCGA group described 4 subtypes of ovarian HGSC, termed “differentiated”, “immunoreactive”, “proliferative”, and “mesenchymal” [19]. Consistently, an earlier study by the Australian Ovarian Cancer Study (ACOS) Group identified subtypes of ovarian HGSC that resemble this classification [20]. Importantly, both studies identified a mesenchymal type of HGSC and demonstrated that this subtype of ovarian HGSC has the worst prognosis [19, 20]. The cell-of-origin of the newly identified mesenchymal type of HGSC is yet to be identified.

In the present study, we designed experiments to explore the role of the Hippo/YAP pathway, a conserved tumor-suppressive pathway, in the differentiation of ovarian granulosa cells. We found that YAP1, the major effector of the Hippo signaling pathway, induced dedifferentiation and reprogramming of ovarian granulosa cells. Unexpectedly, our research results indicated that less-differentiated ovarian granulosa cells could be transformed by hyper-activation of YAP1, leading to the development of tumors with characteristics of the mesenchymal type of HGSC. Our research unveiled a novel potential cell-of-origin of the mesenchymal type of high-grade ovarian carcinoma with serous features.

MATERIALS AND METHODS

Chemicals

DMEM and other cell culture media were purchased from Sigma-Aldrich (St. Louis, MO, USA); fetal bovine serum (FBS) was from Atlanta Biologicals, Inc. (Lawrenceville, GA, USA); Alexa-conjugated secondary antibodies were from Life Technologies™ (Grand Island, NY, USA); YAP1 siRNA#1 and siRNA#2 were from Dhamarcon/Thermo Scientific (Pittsburgh, PA, USA); RNeasy Mini Kit was from QIAGEN Inc. (Valencia, CA, USA); PCR reagents were from Invitrogen (Carlsbad, CA, USA), QIAGEN (Carlsbad, CA, USA) or Bio-Rad (Hercules, CA, USA); antibodies against YAP1, cMyc (Western blot), Sox2, Nanog, Lin28, Klf4, Oct4, E-Cadherin, N-Cadherin (Western blot), Vimentin, Snail, Slug, Claudin1, ZO-1, Cyclin A2, Cyclin B1, Cyclin D1, Cyclin D3, Cyclin E2, PARP, ERBB3, BRCA1, Keratin7, Keratin 20, PAN-Keratin, Aromatase (IHC), cleaved Caspase3, cleaved Lamin A, phosphor-YAP1 (S127), phosphor-LATS1, phosphor-MOB1, phosphor-CREB were from Cell Signaling Technology Inc. (Danvers, MA, USA); antibody against β-actin was from Sigma-Aldrich (St. Louis, MO); Antibodies against Ki67, CA125, cMyc (IHC), and N-Cadherin (IHC) were from Abcam (Cambridge, MA, USA); 3β-HSD antibody was from Ian Mason Ph.D. (Dallas, TX, USA); P450scc antibody was from Millipore (Danvers, MA, USA); Aromatase antibody (Western blot) was from Bio-Rad (Raleigh, NC, USA). Antibodies against PAX2 and PAX8 were from Proteintech (Rosemont, IL, USA); Antibodies against WT1 and AMH were from Santa Cruz (Dallas, TX, USA); Peroxidase-conjugated secondary antibodies for Western blotting were from Jackson Immunoresearch Laboratories Inc. (West Grove, PA, USA); the SuperSignal West Femto Chemiluminescent Substrate Kit was from Pierce/Thermo Scientific (Rockford, IL, USA); and the Optitran® Nitrocellular transfer membrane was from Schleicher&Schuell Bioscience (Dassel, Germany).

Cells and human ovarian tissues

Primary human granulosa cells (hGCs) were collected during oocyte retrieval for *in vitro* fertilization (IVF) at the Heartland Center for Reproductive Medicine (Omaha, Nebraska). The use of human samples was approved by the Institutional Review Board at the University of Nebraska Medical Center. The procedures for the separation of granulosa cells was described previously [21, 22]. HGrC1 cells, an immortalized human granulosa cell line, and KGN cells, an ovarian granulosa cell-like tumor cell line, were obtained from the Riken Biosource Center (Riken Cell Bank, Ibaraki, Japan). Cell lines were validated using short tandem repeat (STR) polymorphism analysis performed by Genetica DNA Laboratories (Burlington, NC, USA). Normal human ovarian tissue slides were obtained from Tianjin Medical University (Tianjin, China). Human ovarian tissues were collected under an approved IRB in the Tianjin Medical University.

Manipulation of YAP1 protein level and activity in granulosa cells

YAP1 protein knockdown was performed with YAP1 targeting siRNA (siRNA#1 and siRNA#2) using protocols described previously [23]. Lipofactamine$^{@}$RNAiMAX Transfection Reagent (Grand Island, NY) was used to deliver siRNA into cells according to the manufacturer's instructions. hGC-YAP, HGrC1-YAP, hGC-YAP^{S127A}, and HGrC1-YAP^{S127A} cell lines were established by transfecting cells with a retrovirus-based YAP1 expressing constructs. hGC-MX and HGrC1-MX were established by transfecting cells with a retrovirus-based control construct (MX). YAP^{S127A} represents mutated YAP1 (serine 127 was replaced with alanine). This S127A mutation prevents the YAP1 protein from being phosphorylated at this site, resulting in its constitutive activity. The cell transfection and screening protocols are described previously [24].

Fluorescent and chromogenic immunohistochemistry/immunocytochemistry

Fluorescent immunohistochemistry was used to localize YAP1, Ki67, 3β-HSD, and cleaved caspase3 proteins in the mouse ovary or 3D culture spheroids. Briefly, frozen sections of 6 μm thickness were fixed in freshly prepared 4% paraformaldehyde and stained for YAP1, Ki67, 3β-HSD, and cleaved caspase3 protein with a protocol established in our laboratory [25]. Images were captured using a Zeiss 710 Meta Confocal Laser Scanning Microscope and analyzed using Zeiss Zen 2010 software (Carl Zeiss Microscopy, LLC, Thornwood, NY). YAP1 and other protein expressions in ovaries and tumor tissues were detected using a peroxidase-based immunohistochemistry assay that was described previously [23]. YAP and Ki67 expression in ascites cells were detected using fluorescent immunocytochemistry as described previously [26].

Three-dimensional hanging drop cell culture

A three-dimensional (3D) hanging drop culture system was employed to determine the role of YAP1 in cell proliferation and cell-cell communication as previously described [27]. Briefly, equal numbers ($0.5X10^{6}$) of hGC-MX, hGC-YAP, hGC-YAP^{S127A}, HGrC1-MX, HGrC1-YAP, HGrC1-YAP^{S127A}, KGN-MX, KGN-YAP, and KGN-YAP^{S127A} cells were loaded onto a GravityPLUS™ 3D Cell Culture plate (InSphero, Schlieren, Switzerland) according to the manufacturer's instructions and incubated for 5 days. Spheroids were

imaged and their sizes were measured using an Olympus inverted microscope (Olympus America, Inc. Center Valley, PA).

Colony formation assays

The role of YAP1 in the transformation was determined using the soft agar assay [28]. Briefly, equal numbers of cells were plated in 0.6% soft agar media and cultured for 10 days. Cells were stained with MTT (3-(4,5-dimethylthiazol-2-yl)-2,5-diphenyltetrazolium bromide). Cell colonies were counted under a bright light microscope. The colony formation results were also confirmed using a semi-quantitative Cytoselect 96-Well Cell Transformation assay kit (Cell Biolabs, Inc., San Diego, CA) according to the manufacturer's instructions.

Tumorigenic studies

To study the tumorigenic activities of the modified HGL5 and HGrC1 cells, equal numbers of HGL5-MXIV, HGL5-YAP^{S127A}, HGrC1-MXIV, HGrC1-YAP^{S127A}, HGrC1-TP53^{R175H}, HGrC1-YAP^{S127A}/TP53^{R175H}, and HGrC1-YAP^{S127A}/TP53^{R175H}/BRCA1$^{-/-}$ cells (10×10^6 cells / 0.1 ml PBS with 0.1 ml Matrigel) were injected subcutaneously (into the dorsal flank) or intraperitoneally into six-week-old female athymic nude mice/NSG mice (NOD.Cg-*Prkdc*^{scid} *Il2rg*^{tm1Wjl}/SzJ, the Jackson Laboratory, 5 – 9 mice/group). Animal experimental procedures were approved by the Institutional Animal Care and Use Committee (IACUC) of the Massachusetts General Hospital and the University at Nebraska Medical Center. OVSAHO cell was used as a positive control. For the subcutaneous xenograft groups, the volume (mm^3) of the tumor was measured and documented every 5 days. Tumor volume = (shortest diameter)^2 × (longest diameter) × 3.14/6. Control and tumor-carrying mice were euthanized and recorded as dead if they showed serious illnesses, such as dysuria, very wasting, sluggishness. Euthanasia was suggested and performed by an experienced veterinarian who had been monitoring these mice and believed that tumor-carrying mice are incurable and suffering more than moderate stress after careful evaluation. Mouse tissues from both studies were collected after euthanasia and processed for preparation of protein and RNA, frozen and paraffin sections for histology and biochemical analyses.

Steroid measurements

Estradiol levels in the cell culture media were monitored using a 17β-Estradiol Enzyme Immunoassay Kit (Arbor Assays, Ann Arbor, Michigan). Progesterone levels in culture medium were determined using a Progesterone ELISA kit (DRG International Inc., Springfield, NJ).

Cell proliferation analysis

Cell numbers were quantified using an Invitrogen Countess automated cell counter [29]. Trypan blue was used to identify and quantify viable cells.

Cell apoptosis assays

Cells were labeled with an Annexin V-FITC Apoptosis Detection Kit (BioVision Inc., San Francisco, CA) following the manufacturer's instructions [26]. Live cells, early apoptotic cells, late apoptotic cells, and dead cells are sorted with flow cytometry at the Flow Cytometry Research Facility at the University of Nebraska Medical Center.

Western blot and RT-PCR analysis

Protein levels were determined by Western blot using a protocol established in our laboratory [23]. Immunosignals were visualized using a Thermo Scientific SuperSignal West Femto Chemiluminescent Substrate Kit (Thermo Fisher Scientific, Rockford, IL). The images were captured and analyzed with a UVP gel documentation system (UVP, LLC, Upland, CA). Expression of mRNA for BCL2, BRIC5, BAX, BAK1, and BAD was detected with quantitative PCR using a protocol previously established in our laboratory [27].

BODIPY staining

Fluorescent neutral lipid dye 4,4-difluoro-1,3,5,7,8-pentamethyl-4-bora-3a,4a-diaza-s-indacene (BODIPY 493/503, green) were used to stain the lipid droplets. Cells or frozen tissues on slides were fixed with 4% paraformaldehyde and washed with PBS for 3 × 5 min. BODIPY, Rhodamine Phalloidin, and DAPI diluted in normal donkey serum were incubated with tissues/cells for 30 min. Wash 3 × 5 min and slides were mounted with Fluoromount-G and coverslips. Pictures were captured using a Zeiss 710 Meta Confocal laser scanning microscopy.

Hematoxylin and Eosin stain for histology analyses

Mouse xenografts were harvested and fixed with formalin. After paraffin-embedding and section, Hematoxylin and eosin (H&E) stain was performed for xenograft tissue slides. Histology analyses were conducted by the pathologist Dr. Yun-An Tseng at the University of Nebraska Medical Center.

Array Comparative Genomic Hybridization (aCGH).

Genomic DNA was extracted from xenografts, cultured ascites cells, and control HGrC1 cells. DNA samples were hybridized with normal reference DNA to the Cancer Microarray (Agilent 180K CGH+SNP Array, CCMC design, GRCh37) to perform aCGH profiling. This array targets genes associated with cancer at 5–10 kb copy number resolution and provides 25 kb whole genome copy number coverage for precise breakpoint delineation. Copy number changes > 500 kb in size and copy-neutral loss of heterozygosity (LOH) will be reported.

DNA Methylation analysis

DNA was extracted from cultured cells or tissues. Illumina methylation EPIC 850k array was performed to assess methylation at approximately 850,000 CpG sites of DNA (University of Nebraska Medical Center (UNMC) Epigenomics Core). RnBeads was used to analyze the methylome data, and our analysis was restricted to CpG methylation.

Statistical analysis

All experiments were repeated at least three times unless otherwise noted. Statistical analyses were conducted with GraphPad Prism software (GraphPad Software, Inc.). Data were analyzed for significance by student T-test or by one-way ANOVA with Tukey's post-hoc test as indicated. A value of $P < 0.05$ was considered to be significant.

RESULTS

Differential expression of YAP1 in the mouse and human ovarian granulosa cells

Our previous data showed that YAP1 is highly expressed in transformed granulosa cells [24]. The expression of YAP1 during granulosa cell differentiation and follicle development in mammals has not been thoroughly examined. Using fluorescent immunohistochemistry analyses, we found that YAP1 protein was mainly expressed in granulosa and luteal cells of the adult mouse ovary (Fig. 1). Interestingly, the expression and localization of YAP1 varied with granulosa cell differentiation. In growing follicles, granulosa cells are highly proliferative, which is indicated by the high expression of Ki-67 (Fig 1b, 1e), and less differentiated, which is indicated by the negative expression of 3β-HSD (Fig. 1c, 1f). YAP1 is predominantly expressed in the nuclei of these proliferative granulosa cells (Fig. 1a, 1d). However, in the corpus luteum, granulosa cells are luteinized and terminally differentiated (indicated by the negative expression of Ki-67 and very high expression of 3β-HSD, Fig. 1b, 1e, 1c, 1f). YAP1 is mainly localized to the cytoplasm of luteinized granulosa cells (Fig. 1a, 1d). Importantly, this shift is not just observed in the mouse model. In the human ovarian granulosa cells, YAP1 expression is also associated with cell growth and differentiation (Fig. 1g, 1h). Furthermore, expression of LATS1/2, the upstream suppressors of YAP1, was elevated in luteinized granulosa cells compared with proliferative granulosa cells (Fig. 1i, 1j), supporting the shift of YAP1 expression between granulosa cells and luteal cells. Since nuclear YAP1 is the active form [30, 31], the shift of YAP1 localization during granulosa cell growth and differentiation indicates that the expression of YAP1 protein is tightly associated with granulosa cell proliferation and differentiation.

YAP1 promotes proliferation, supports survival, but disrupts steroidogenesis of human granulosa cells

Nuclear localization of YAP1 indicated that YAP1 might regulate the proliferation of granulosa cells. To examine the role of the endogenous YAP1 in granulosa cell proliferation, we knocked down YAP1 expression in primary cultures of hGCs from IVF patients using YAP1-targeting siRNAs (siRNA 1 and 2). Knockdown of YAP1 in hGCs significantly suppressed cell proliferation (Fig. 2a). Annexin V-base flow cytometry showed that YAP1 knockdown also increased cell apoptosis (Fig. 2b). To further verify the role of YAP1 in granulosa cell proliferation and differentiation, we ectopically expressed YAP1 protein in hGCs using a retrovirus-based ectopic gene expression system. hGC-MX cells were generated by transfecting hGCs with an empty vector (MXIV) and were used as a control. hGC-YAP cells were generated by transfecting hGCs with a MXIV-derived vector expressing wild type YAP1. hGC-YAP^{S127A} cells were generated by transfecting hGCs with a MXIV-derived vector expressing constitutively active YAP1 (YAP^{S127A}, Serine 127 was mutated to Alanine to avoid inhibition by LATS phosphorylation [32, 33]). Western blot

analyses showed that both hGC-YAP and hGC-YAP^{S127A} cells expressed a high level of YAP1 (Fig. 2c). Cell proliferation analyses showed that ectopic expression of both wild-type or constitutively active YAP1 stimulated the growth of hGCs (Fig. S1a online). To mimic the growth of granulosa cells *in vivo*, we established a 3D hanging-drop culture system, in which hGCs establish natural cell-cell contact to form a spheroid structure, similar to granulosa cell growth in the ovarian follicle [34, 35]. Consistent with results obtained from traditional cell culture, ectopic expression of YAP1 in hGCs also stimulated cell growth in the 3D culture system, which is indicated by the significant increase in the volume of spheroids formed by hGC-YAP and hGC-YAP^{S127A} groups compared to the control group ($P < 0.01$, Fig. 2c). Treatment of hGCs with Verteporfin, a selective antagonist of YAP1 activities [36], blocked cell growth, induced gradual destruction of the spheroids in all examined groups. Fluorescent immunocytochemistry showed verteporfin eliminated YAP1-stimulated Ki-67 positive cells and induced expression of cleaved caspase-3 in both hGC-MX and hGC-YAP^{S127A} cells in the 3D-culture system (Fig. S1b, c online). Importantly, we observed that the ectopic expression of YAP1 was able to induce anchorage-free growth of luteinized hGCs (Fig. S2a–c online), suggesting that YAP1 may be able to induce transformation of granulosa cells.

The ability of YAP1 to stimulate granulosa cell proliferation and survival was further confirmed using the KGN cell line, which is a luteinized granulosa-cell like tumor cell line with characteristics of late-stage granulosa cells [37]. Flow cytometry showed that ectopic expression of YAP1 or YAP^{S127A} in KGN cells promoted cell cycle progression under either serum-free or serum-supplemented culture conditions (Fig. S3a online), and significantly reduced the number of starvation-induced apoptotic cells (Fig. S4a, 4b online). Ectopic expression of YAP1 also enhanced KGN cell growth in a 3D hanging-drop culture system (Fig. S3c online). Biochemical analyses showed that ectopic expression of YAP1 in KGN cells induced expression of Cyclin A2, B1, D1, D3, and E2, (Fig. S3b online), increased mRNA level of *Bcl2* and *Bric5*, and decreased the expression of pro-apoptotic genes including *Bax*, *Bad*, and *Bak1* (Fig. S4c online). Consistently, verteporfin, the antagonist of YAP1 protein, suppressed KGN cell proliferation (Fig. S5a online), reduced proliferation markers cyclin D1 and c-MYC, and enhanced markers of apoptosis, e.g., cleaved Lamin A, cleaved PARP and cleaved caspase-3 in a concentration-dependent manner (Fig. S5b online).

A major feature of differentiated granulosa cells is their ability to secret female sex hormones, such as 17β-estradiol (E2) and progesterone (P4) [38–40]. Follicle-stimulating hormone (FSH), via activating the adenylate cyclase and subsequently the PKA signaling pathway, serves as a major regulator of granulosa cell differentiation and steroidogenesis [41, 42]. FSH activated the Hippo pathway within 10 minutes in KGN cells, which is indicated by the significant increase in the phosphorylation of LATS1/2, leading to YAP1 phosphorylation (Fig. S6a online). FSH increased E2 and P4 secretion and suppressed cell proliferation (Fig. S6c, 6d online). Forskolin (FSK), a selective activator of adenylate cyclase that has been frequently employed to mimic FSH action in granulosa cells, also activated the Hippo pathway, suppressed YAP1 activity, induced E2 and P4 secretion, and suppressed proliferation in KGN cells (Fig. S6a, 6d online). Although FSK significantly increased production of E2 and P4 in the hGC-MX cells, its effect on the E2 and P4 secretion in hGCs and KGN cells was significantly compromised in hGC-YAP and

hGC-YAP^{S127A} cells (Fig.2d). Consistent with this, expression of YAP1 or YAP^{S127A} in hGCs suppressed FSK-induced transcription of *CYP19A1* and *CYP11A1* genes (Fig.2e). Similarly, ectopic expression of YAP1 or YAP^{S127A} in KGN cells almost eliminated basal and FSH- or FSK-stimulated E2 and P4 production, and greatly suppressed FSH- and FSK-stimulated expression of P450 SCC and aromatase, two key enzymes to produce sex hormones (Fig. 2f, 2g).

YAP1 induces de-differentiation and reprogramming of hGCs

YAP1 induces proliferation and suppresses steroidogenesis and expression of steroidogenic enzymes, implying that YAP1 may induce the de-differentiation of granulosa cells. To verify this hypothesis, we examined the expression of FSHR and LHCGR, two important differentiation markers of granulosa cells, in highly differentiated hGCs. Real-time PCR showed that ectopic expression of YAP1 or YAP^{S127A} significantly suppressed expression of FSHR and LHCGR, but greatly induced expression of the MYC gene, a known marker of cell stemness (Fig. 3a). In the ovary, well-differentiated lutein cells are featured with an accumulation of lipid droplets (Fig. 3b). Ectopic expression of YAP1 or YAP^{S127A} in KGN cells eliminated the FSK-induced increase of lipid droplet accumulation in cells. These data demonstrate that YAP1, indeed, blocks the differentiation of granulosa cells (Fig. 3c). Supporting this notion, we found that ectopic expression of YAP1 or YAP^{S127A} in KGN cells suppressed almost all granulosa cell differentiation markers, including *FSHR, INHA, INHBB, CYP19A1, CYP11A1,* and *PLN2*, but significantly increased expression of stemness markers such as *TERT* and *MYC* (Fig. 3d). YAP1 stimulating expression of *TERT* and *MYC,* two cell stemness associated genes, suggests that YAP1 not only dedifferentiates granulosa cells but may also induce reprogramming of granulosa cells. Consistent with this hypothesis, we found that ectopic expression of YAP1 or YAP^{S127A} in KGN cells up-regulated critical cell reprogramming factors, such as c-Myc, Sox2, Nanog, and Lin28 (Fig. 3e). In addition, we found that hyper-activation of YAP1 in granulosa cell-like KGN cells resulted in mesenchymal to epithelial transition (MET), which is indicated by the decreases in the protein levels of vimentin, snail, slug (mesenchymal cell markers) and increases in claudin 1 and ZO-1 (epithelial cell markers, Fig. 3f). Recent studies indicate that MET is a vital process for successful reprogramming of somatic cells [43, 44], further supporting our hypothesis that YAP1 is able to induce de-differentiation and reprogramming of granulosa cells.

Since YAP1 induced de-differentiation and reverted the highly differentiated granulosa cells into poorly differentiated granulosa cells, we used a less-differentiated granulosa cell line, HGrC1 cell, to further evaluate the role of YAP1 in poorly differentiated (less-differentiated) granulosa cells. HGrC1 is an immortalized human granulosa cell line established from granulosa cells isolated from healthy growing follicles, and is the only existing cell line with characteristics of granulosa cells in the early stage of ovarian follicle growth [45]. As described above, we established HGrC1-MX (control), HGrC1-YAP (expressing wild-type of YAP1), and HGrC1-YAP^{S127A} cells (expressing constitutively active YAP1) and found that ectopic expression of YAP1 or YAP^{S127A} accelerated proliferation of HGrC1 (Fig. S7a online). Consistently, knockdown of YAP1 in HGrC1 cells significantly suppressed cell proliferation (Fig. S7b online). Similarly, in the 3D hanging drop culture system,

both YAP1 and or YAP^{S127A} promoted the proliferation and survival of HGrC1 cells (Fig. S7c–e online). In the soft agar assay, HGrC1-MX formed very few small colonies, whereas HGrC1-YAP and HGrC1-YAP^{S127A} cells formed many large colonies (Fig. S8a–b online). These data further indicate that Hyperactivation of YAP1 may support anchorage-independent survival and induce malignant transformation in less-differentiated granulosa cells.

To further confirm our observations, we analyzed gene expression profiles of HGrC1-MX, HGrC1-YAP^{S127A}, KGN-MX, and KGN-YAP^{S127A} cells using RNA-seq. Based on the RNA-seq data, we performed the gene set enrichment analysis (GSEA). GSEA analyses showed that, consistent with our above observations, genes-associated with granulosa cell differentiation (such as steroidogenic gene sets) and epithelial-mesenchymal transition (EMT) were down-regulated, while genes-associated with cellular stemness and pluripotency are significantly enriched in both HGrC1 and KGN cells (Fig. 3g, Fig. S9–10 online). The results derived from the high throughput analyses strongly strengthened our conclusion that YAP1 not only dedifferentiates granulosa cells but also induces reprogramming of these cells.

Hyperactivation of YAP1 induced high-grade metastatic ovarian cancer with serous features from less-differentiated granulosa cells.

Under physiological conditions, ovulation may introduce well-differentiated granulosa cells into the peritoneal cavity. These differentiated granulosa cells cannot survive without ECM attachment. As shown above, we found that granulosa cells with hyperactivated YAP1 could be de-differentiated and reprogrammed, and developed the ability to grow in an attachment-free manner. We hypothesize that under certain pathological conditions, constitutive activation of YAP1 may occur in ovarian granulosa cells and induce de-differentiation, reprogramming and transformation of these cells, leading to their continuous proliferation in the peritoneal cavity. To examine this hypothesis, HGrC1-MX (control) and HGrC1-YAP^{S127A} cells were injected intraperitoneally into the immunodeficient mice to examine their survival ability. As expected, HGrC1-MX cells did not grow and disappeared in the peritoneal cavity. However, HGrC1-YAP^{S127A} cells grew very well in the pelvic and formed metastatic cancers (Fig. 4). Tumors derived from HGrC1-YAP^{S127A} cells progressed very slowly in the early stage. Once the tumor progressed to a certain stage, large volume of ascites was observed in these mice, and these animals die several weeks after the appearance of ascites (Fig. 4a). These tumors were very aggressive and metastasized to the omentum visceral fat tissue, gastrointestinal system, diaphragm, liver, pancreas, and spleen (Fig. 4b). Tumor cells isolated from ascites express high YAP1 and Ki-67 protein. The nuclei of these ascites cells are highly pleomorphic and larger with coarsely clumped chromatin (Fig. 4c). Histology studies showed that cancer cells in tumor tissues are generally intermediate to large in size with prominent nucleoli at low magnification (Fig. 4d). The nuclei are distinctly pleomorphic, showing more than a threefold variation in size. These cells are very proliferative, which is indicated by the frequent appearance of mitotic figures (Fig. 4d). Cancer cells aggressively invaded into almost all organs and tissues in the peritoneal cavity (Fig. 4b, 4d). The histopathological feature of these cancers derived from YAP1-reprogrammed granulosa cells is more like High grade serous ovarian cancers.

HGL5 cell is an immortalized granulosa cell line that was originally from luteinized granulosa cells collected from an IVF patient during oocyte retrieval procedures [46]. These cells retained many characteristics of luteinized (well-differentiated) granulosa cells. For example, these cells express steroidogenic enzymes and have the ability to produce estrogen and progesterone in response to cAMP and Forskolin stimulation. To verify if YAP1 can also induce tumorigenesis in the well-differentiated granulosa cells, we established HGL5-MX and HGL5-YAP^{S127A} cell lines. We found that hyperactivation of YAP1 in HGL5 cells also induced significant nuclear pleomorphism and greatly stimulate cell proliferation (Fig. S11, 12a online). When implanted subcutaneously into the NSG mice, HGL5-MX cells did not form any tumor. However, HGL5-YAP^{S127A} cells formed tumors that histologically resemble those derived from HGrC1-YAP^{S127A} cells (Fig. S12b–d online).

BRCA1 inactivation, not TP53 mutation, promoted YAP-induced malignant transformation of granulosa cells

It is known that TP53 and BRCA1/2 are two major contributors to ovarian high grade serous cancers [47]. TP53 participates in processes involving de-differentiation and cell reprogramming [48–50] and is mutated in almost all ovarian high grade serous cancers [47]. BRCA dysfunction contributes to the development of almost 50% ovarian high grade serous carcinoma [47]. Although a tumorigenic gain-of-function activity of mutated TP53 has been frequently reported [51–53], *in vitro* studies showed that compared to control HGrC1 cells, the introduction of mutated TP53 (TP53^{R175H}) in HGrC1 cells (HGrC1-TP53^{R175H} cells) or HGrC1-YAP^{S127A} (HGrC1-YAP^{S127A}/TP53^{R175H} cells) had no effect on the formation of colonies. However, inactivation of *BRCA1* in HGrC1-YAP^{S127A}/TP53^{R175H} cells (HGrC1-YAP^{S127A}/TP53^{R175H}/BRCA1$^{-/-}$ cells) significantly increased colony formation ($P < 0.001$, Fig. 5a–b). Consistent with the *in vitro* studies, intraperitoneal injection of HGrC1-TP53^{R175H} cells into NSG mice did not form tumors. The introduction of TP53^{R175H} also did not affect the progression of tumors derived from HGrC1-YAP^{S127A} cells (Fig. 5c and Fig. S13 online). However, inactivation of the *BRCA1* gene in the HGrC1-YAP^{S127A}/TP53^{R175H} cells (HGrC1-YAP^{S127A}/TP53^{R175H}/BRCA1$^{-/-}$ cells) induced development of more aggressive metastatic cancers. BRCA1 inactivation significantly shortened the time of tumor progression, hastened the onset of death and greatly reduced the survival rate of mice carrying tumors from the cells. (Fig. 5c–d). Similar to tumors derived from HGrC1-YAP^{S127A} cells, histological studies showed that tumors derived from HGrC1-YAP^{S127A}/TP53^{R175H}/BRCA1$^{-/-}$ cells resemble high-grade ovarian carcinoma. (Fig. 5e).

Hyperactivation of YAP1 induced mesenchymal type of high-grade ovarian cancer with serous features from less-differentiated granulosa cells.

Consistent with the very high mitotic index, immunohistochemistry analysis showed that Ki-67 is highly expressed in tumor tissues derived from the HGrC1-YAP^{S127A}/TP53^{R175H}/BRCA1$^{-/-}$ cells (Fig. 6a). Moreover, the majority of known biomarkers for ovarian HGSCs, such as nuclear TP53, PAX-8, WT-1, MYC, KRT7 (cytokeratin-7), as well as pan-keratin, were highly expressed in tumors derived from these cells (Fig. 6a). Accordingly, granulosa cell tumor markers such as aromatase (CYP19A1) and AMH (Mullerian inhibiting substance) were not expressed in these tumors (Fig. 6b). The morphological features and negative expression of PAX-2 in these tumor tissues indicated that these are not LGSCs (Fig.

6c). In addition, the negative PAS staining (positively stained in the positive intestine cells in the same slide) and KRT 20 (keratin 20) suggested that these tumors are not mucinous cancers (Fig. 6c–d). The molecular features of these tumor tissues clearly indicate that these tumors resemble HGSC. Interestingly, these tumor cells retain some mesenchymal features. For example, they have a very high expression of N-cadherin, but not E-cadherin (Fig. 6e). These tumors also had no (or very low, if any) expression of Muc16 (CA125) (Fig. 6e). Similar molecular characteristics were observed from tumor tissues derived from HGrC1-YAP^{S127A} cells and HGrC1-YAP^{S127A}/TP53^{R175H} cells (Fig. S14 online). Expression of these markers was further verified in the established cell lines (HGrC1-Ctrl cells, HGrC1-TP53^{R175H} cells, HGrC1-YAP^{S127A} cells, HGrC1-YAP^{S127A}/TP53^{R175H} cells, and HGrC1-YAP^{S127A}/TP53^{R175H}/BRCA1$^{-/-}$ cells.), and ascites cancer cells derived from mice carrying tumors from HGrC1-YAP^{S127A} cells, HGrC1-YAP^{S127A}/TP53^{R175H} cells, and HGrC1-YAP^{S127A}/TP53^{R175H}/BRCA1$^{-/-}$ cells (Fig. 6f).

One of the most important features of ovarian HGSC is genome instability. We performed aCGH analyses to determine whether disruption of the Hippo pathway also affects genome instability in granulosa cells. The results showed that the hyper-activation of YAP1 in less-differentiated granulosa cells induced considerable genome instability in these cells, which is evidenced by the frequent fragment amplifications and deletions observed in tumor tissues and ascites cancer cells derived from the HGrC1-YAP^{S127A}, HGrC1-YAP^{S127A}/TP53^{R175H}, and HGrC1-YAP^{S127A}/TP53^{R175H}/BRCA1$^{-/-}$ cells implanted mice (Fig. 7a). Gene deletions mainly occurred in chromosomes 4, 13, 14, 15, and X. Numerous copy number gains were evident in other chromosomes (Fig. 7a). Based on the high-throughput analysis of the genome-wide DNA methylation, both principal component analysis and the dendrogram classification analysis showed that HGrC1-YAP^{S127A} cells, fallopian tube epithelial cells, and OSE cells have the closest relationship with human ovarian HGSC compared to other cancer cell lines (Fig. 7b–c). These results provide strong genome-wide epigenetic evidence that less-differentiated granulosa cells could be reprogramed and transformed by hyperactivation of YAP1 to initiate a mesenchymal subtype of high-grade ovarian cancers.

DISCUSSION

The Hippo/YAP pathway is a conserved signaling pathway that controls tissue homeostasis during development by regulating cell proliferation, differentiation and survival [32, 54–57]. Accumulating evidence indicates that the Hippo/YAP pathway plays a critical role in tumorigenesis [27, 58–60]. Our previous studies indicated that the Hippo/YAP signaling pathway interacts with the EGFR signaling pathway to drive the tumorigenesis of OSE cells [27]. We also found that YAP1, the major effector of the Hippo tumor-suppressive pathway, plays a critical role in the malignant transformation of the fallopian tube secretory epithelial cells [61], which have been recently identified as a major cell-of-origin for ovarian HGSC [6–9, 18, 47]. In the present study, our research results show that YAP1 is a major regulator of proliferation and differentiation of ovarian granulosa cells. In the undifferentiated or less differentiated granulosa cells, YAP1 is mainly expressed in the nucleus. In the terminally differentiated granulosa cells (or lutein cells), YAP1 is predominantly expressed in the cytoplasm. Ectopic expression of YAP1 in the highly differentiated granulosa cells results in the dedifferentiation of these cells, which is indicated by the loss of their

specialized functions, such as expression of steroidogenic enzymes, production of estrogen and progesterone, and secretion of inhibins. Ectopic expression of YAP1 also results in a significant increase in expression of cellular reprogramming factors such as MYC, Nanog, Lin28, and Sox2. Moreover, hyperactivation of YAP1 in granulosa cells induces expression of epithelial markers such as ZO-1 and claudin-1, but greatly suppresses expression of mesenchymal cell markers such as vimentin, snail, and slug, indicating the initiation of MET in these cells. It is known that the initial step of cell reprogramming is featured by MET [43, 44]. Enhanced expression of cellular reprogramming factors and mesenchymal-epithelial transition in granulosa cells with constitutively active YAP1 suggest that hyperactivation of YAP1 results in reprogramming of granulosa cells. These observations are consistent with previous reports that YAP1 is critical for the maintenance of cell pluripotency [62–65]. A more recent study showed that high expression of YAP1 induced stem cell-like cell populations in differentiated mammary gland cells, fetal neurons, and pancreatic exocrine cells [66]. To our knowledge, this is the first report showing hyper-activation of YAP1 in the granulosa cells results in dedifferentiation, reprogramming, and transformation of these specialized ovarian cells.

The significance of YAP-induced de-differentiation / reprogramming of the granulosa cell is not documented. Under physiological conditions, monthly ovulation results in the insemination of well-differentiated granulosa cells into the peritoneal cavity of women at the reproductive age. These differentiated granulosa cells eventually die because they cannot survive without ECM attachment. Under certain pathological conditions, however, constitutive activation of YAP1 may occur in granulosa cells and induce de-differentiation, reprogramming and malignant transformation of granulosa cells. As shown above, these de-differentiated / reprogrammed granulosa cells with hyperactivated YAP1 can grow in an anchorage-free manner and develop/transdifferentiate into high grade ovarian cancer with serous features in the peritoneal cavity. Supporting our hypothesis, we found that the HGrC1 cell line, which is the only existing poorly differentiated granulosa cell line established from granulosa cells of healthy human growing follicles, could not survive in mouse peritoneal cavity. However, intraperitoneal implanted HGrC1-YAP^{S127A} cells not only survive and proliferate in the mouse peritoneal cavity but also induced highly metastatic tumors in the immunodeficient mice. The presence of tumor cells induced a large amount of ascites in the peritoneal cavity. These tumor cells were invasive and metastasized to the omentum, gastrointestinal system, visceral fat tissue, diaphragm membrane, liver, pancreas, and muscle tissues. Histological studies showed that the nuclei of these tumor cells are highly pleomorphic and larger with coarsely clumped chromatin. Moreover, these tumor tissues have a very high mitotic index, including many abnormal mitotic figures. Furthermore, cultured tumor cells derived from the ascitic fluid are very proliferative and featured with the nuclear atypia. In addition, almost all known biomarkers for ovarian HGSCs, such as high Ki-67, PAX-8, WT-1, Keratin-7, as well as Pan-Keratin, are highly expressed in the cancer cells derived from HGrC1-YAP^{S127} mice, HGrC1-YAP^{S127A}/TP53^{R175H} mice, and HGrC1-YAP^{S127A}/TP53^{R175H}/BRCA1$^{-/-}$ mice. The morphological features and negative expression of PAX-2 in these tumor tissues suggest that these are not LGSCs. The negative PAS staining and negative keratin 20 suggests that these tumors are not mucinous cancers. The molecular feature of these tumor tissues indicated that these tumors are high-grade

ovarian carcinoma with serous features. These observations strongly support the notion that hyperactivated YAP1 induce malignant transformation of less-differentiated granulosa cells, leading to the development of high grade ovarian cancer with serous feature, not benign granulosa cell tumor.

Granulosa cell is a known mesenchymal type of ovarian cells. iPSCs induced from hGCs are able to differentiate into osteoblast, muscle cells, and neurons, which are all mesenchymal type of cells. It has also been shown that a subpopulation of granulosa cells within the growing follicle (less differentiated granulosa cells) possesses exceptional plasticity. Mouse ovarian progenitor granulosa cells express Lgr5, which is a stem cell marker of stem/progenitor cells of the ovary and tubal epithelia [67–69]. Isolated granulosa cells express stem cell markers, have high telomerase activity, and are able to differentiate into other cell types otherwise not present within ovarian follicles [70–72]. Although we observed obvious decreased mesenchymal cell markers and increased epithelial markers after ectopic expression of YAP1 in HGrC1 cells, the tumor cells derived from HGrC1-YAP^{S127A} cells kept their mesenchymal lineage. These cancer cells express high levels of N-cadherin and vimentin, but undetectable E-cadherin. Moreover, these tumors have low to no expression of CA-125. Interestingly, the AOCS gene expression profiling study identified a subtype of high grade serous ovarian cancer exhibited a signature that featured many genes involved in mesenchymal development. These cancer cells have a high level of N-cadherin, but a very low or undetectable level of E-cadherin [20]. This type of HGSC also has no or low expression of CA-125 [20]. Since CA-125 is typically expressed in the epithelial and mesothelial type of cells, the minimal expression of CA-125 in the mesenchymal HGSC further reflects the dedifferentiated/mesenchymal feature of this subtype of high grade serous ovarian cancer. The existence of a mesenchymal subtype HGSC in human patients has been confirmed by TCGA [19]. Of importance herein, both groups demonstrated that this subtype of ovarian HGSC had the worst prognosis [19, 20]. Due to its mesenchymal molecular features, the cell-of-origin for the newly identified mesenchymal type of HGSC remains unknown. Based on the mesenchymal lineage, histological and molecular features, we speculate that reprogrammed ovarian granulosa cells could be a potential cell-of-origin of the most lethal mesenchymal type of ovarian HGSC. Importantly, hyperactivation of YAP1-induced reprogramming and trans-differentiation of granulosa cells provides an alternative explanation for the high genomic heterogeneity observed in epithelial ovarian cancers.

The mechanism by which YAP1 induces HGSC with serous-like features and mesenchymal lineage from granulosa cells needs further studies. However, we found YAP1 was capable of inducing chromosome instability in less-differentiated granulosa cells. Constitutive activation of YAP1 induced frequent chromosome aberrations. The major change was the deletion of genes in chromosomes 4, 13, 14, 22, and chromosome X and gain of fragments in many other chromosomes. Although the exact molecular events by which YAP1 induce chromosome instability is still unclear, we noticed that hyperactivation of YAP1 consistently induced deletion of DNA fragments in chromosome 13, which harbors several critical tumor suppressor genes such as *BRCA2*, *RB1,* and *LATS2*. The tumorigenic role of inactivation of these tumor suppressors has been well-studied. Moreover, our data showed that YAP1 induced expression of cell reprogramming factors such as MYC and SOX2. It has been

reported that cell reprogramming factors have the potential to induce genome instability [48]. Therefore, DNA damage response pathways might be a potential link between YAP1-induced cell reprogramming and tumorigenesis.

TP53 plays a critical role in the cellular DNA damage response process to protect cells from any potential inherited chromosomal aberrations during the process of de-differentiation [48, 50]. The abrogation of TP53 leads to persistent DNA damage and chromosomal aberrations during cell reprogramming [48, 49]. Importantly, recent data showed that mutated *TP53* could promote tumor progression via gain-of-function mutations [51, 52], further supporting the importance of TP53 in the development of ovarian HGSC. Importantly, *TP53* is mutated in the majority of patients with ovarian HGSC [47]. The introduction of $TP53^{R175H}$ alone had no effect on chromosomal stability, tumorigenesis, and tumor-carrying mouse survival, suggesting that the previously observed gain-of-function effect is not exerted in the HGrC1 cells.

BRCA1/2 are also critical for maintaining genome stability [73, 74]. Abnormal inactivation of *BRCA1/2* genes was believed to contribute to the development of > 50% of ovarian HGSC [47]. In the present study, we found that inactivation of BRCA1 significantly enhanced YAP1-induced malignant transformation of HGrC1 cells, promoted tumor progression, and greatly reduced survival of tumor-carrying mice, suggesting that BRCA1 gene plays a critical role in YAP1-induced tumorigenesis of granulosa cells. BRCA1 may be one of the important factors that are involved in the initiation and progression of the mesenchymal subtype of HGSC. As shown in this study, YAP1 induced granulosa cell dedifferentiation and reprogramming, two processes that frequently induce DNA damages and chromosomal instability [75, 76]. It is very possible that high YAP1 may induce DNA damage in granulosa cells. Inactivation of BRCA1 genes in these cells would result in the failure of DNA damage repair and development of genome instability, leading to the accumulated chromosomal instability and tumorigenesis. Therefore, the development of a mesenchymal subtype of HGSC may be attributed to the combined actions of YAP1 hyper-activation and BRCA1 inactivation.

In conclusion, we found that hyperactivation of YAP1 induced de-differentiation / reprogramming and malignant transformation of ovarian granulosa cells, leading to the development of high grade ovarian cancer with mesenchymal lineage and serous feature. Although epidemiological studies showed that ovulation frequency is closely associated with epithelial ovarian cancer incidence, the intrinsic connection between these two physiological/pathological events is unclear. Research results in this study provide the first evidence for the direct linkage between ovulation and epithelial ovarian cancer incidence. Most importantly, genomic and epigenetic heterogeneity has been blamed, in part, for the poor prognosis of the ovarian HGSC because it reduces the likelihood of finding a single therapy that is effective for the majority of patients. In the present study, we showed that dedifferentiated/reprogrammed granulosa cells may serve as cell-of-origin of the ovarian HGSC with mesenchymal features. Hyperactivation of YAP1 is a major driver of malignant transformation of the less-differentiated granulosa cells. These findings not only provide a new explanation for the existing ovarian cancer heterogeneity but also unveils the cellular

and molecular target for the prevention, early diagnosis and personalized treatment of a new subtype of high grade serous ovarian cancer.

Supplementary Material

Refer to Web version on PubMed Central for supplementary material.

ACKNOWLEDGMENT

This work was supported by the National Cancer Institute / the National Institute of Health (1R01CA197976, 1R01CA201500), the Vincent Memorial Hospital Foundation / the Vincent Center for Reproductive Biology, the Olson Center for Women's Health; University of Nebraska Medical Center Graduate Studies Fellowship; the Fred & Pamela Buffett Cancer Center (LB595); Colleen's Dream Foundation; the Marsha Rivkin Center for Ovarian Cancer Research (the Barbara Learned Bridge Funding Award), and the CoBRE grant from the Nebraska Center for Cellular Signaling/ the National Institute of General Medical Science/the National Institute of Health (5P30GM106397). We thank the Bioinformatics and Systems Biology Core at UNMC for providing genome-wide methylation profiling analysis services, which receives support from the Nebraska Research Initiative (NRI) and NIH (2P20GM103427 and 5P30CA036727). We thank Janice A. Taylor and James R. Talaska of the Advanced Microscopy Core Facility at the University of Nebraska Medical Center for providing assistance with confocal microscopy. We also thank Philip Hexley and Victoria B. Smith of The Flow Cytometry Research Facility at the University of Nebraska Medical Center for providing assistance with flow cytometry.

作者简介和图片

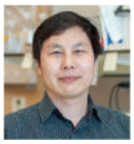

Cheng Wang is an Investigator at Massachusetts General Hospital and an Associate Professor at Harvard Medical School. Dr. Wang obtained his B.S. and Ph.D. from Nanjing Agriculture University. Research in his laboratory mainly focuses on uncovering the cellular and molecular mechanisms underlying the development of cancers in female reproductive organs, aiming to improve the prevention, early diagnosis, and treatment of these malignancies.

Xiangmin Lv is a Post-doctoral Research Fellow at Massachusetts General Hospital and Harvard Medical School. He obtained his B.S. from SouthWest JiaoTong University and Ph.D. from the University of Nebraska Medical Center in the US. His research focuses on cancer biology and the Hippo/YAP signaling pathway.

REFERENCES

[1]. Jemal A, Bray F, Center MM, et al. Global cancer statistics. CA Cancer J Clin 2011; 61, 69–90. [PubMed: 21296855]

[2]. Vang R, Shih Ie M, and Kurman RJ. Ovarian low-grade and high-grade serous carcinoma: pathogenesis, clinicopathologic and molecular biologic features, and diagnostic problems. Adv Anat Pathol 2009; 16, 267–82. [PubMed: 19700937]

[3]. Li J, Fadare O, Xiang L, et al. Ovarian serous carcinoma: recent concepts on its origin and carcinogenesis. J Hematol Oncol 2012; 5, 8. [PubMed: 22405464]

[4]. Seidman JD, Horkayne-Szakaly I, Haiba M, et al. The histologic type and stage distribution of ovarian carcinomas of surface epithelial origin. Int J Gynecol Pathol 2004; 23, 41–4. [PubMed: 14668549]

[5]. Selvaggi SM Tumors of the ovary, maldeveloped gonads, fallopian tube, and broad ligament. Arch Pathol Lab Med 2000; 124, 477. [PubMed: 10705419]

[6]. Karnezis AN, Cho KR, Gilks CB, et al. The disparate origins of ovarian cancers: pathogenesis and prevention strategies. Nat Rev Cancer 2017; 17, 65–74. [PubMed: 27885265]

[7]. Levanon K, Crum C, and Drapkin R. New insights into the pathogenesis of serous ovarian cancer and its clinical impact. J Clin Oncol 2008; 26, 5284–93. [PubMed: 18854563]

[8]. Dubeau L The cell of origin of ovarian epithelial tumors and the ovarian surface epithelium dogma: does the emperor have no clothes? Gynecol Oncol 1999; 72, 437–42. [PubMed: 10053122]

[9]. Kurman RJ Origin and molecular pathogenesis of ovarian high-grade serous carcinoma. Ann Oncol 2013; 24 Suppl 10, x16–21. [PubMed: 24265397]

[10]. Piek JM, van Diest PJ, Zweemer RP, et al. Dysplastic changes in prophylactically removed Fallopian tubes of women predisposed to developing ovarian cancer. J Pathol 2001; 195, 451–6. [PubMed: 11745677]

[11]. Perets R, Wyant GA, Muto KW, et al. Transformation of the fallopian tube secretory epithelium leads to high-grade serous ovarian cancer in Brca;Tp53;Pten models. Cancer Cell 2013; 24, 751–65. [PubMed: 24332043]

[12]. Dubeau L and Drapkin R. Coming into focus: the nonovarian origins of ovarian cancer. Ann Oncol 2013; 24 Suppl 8, viii28–viii35. [PubMed: 24131966]

[13]. Klinkebiel D, Zhang W, Akers SN, et al. DNA Methylome Analyses Implicate Fallopian Tube Epithelia as the Origin for High-Grade Serous Ovarian Cancer. Mol Cancer Res 2016; 14, 787–94. [PubMed: 27259716]

[14]. Shih Ie M, Chen L, Wang CC, et al. Distinct DNA methylation profiles in ovarian serous neoplasms and their implications in ovarian carcinogenesis. Am J Obstet Gynecol 2010; 203, 584 e1–22. [PubMed: 20965493]

[15]. Dehari R, Kurman RJ, Logani S, et al. The development of high-grade serous carcinoma from atypical proliferative (borderline) serous tumors and low-grade micropapillary serous carcinoma: a morphologic and molecular genetic analysis. Am J Surg Pathol 2007; 31, 1007–12. [PubMed: 17592266]

[16]. Boyd C and McCluggage WG. Low-grade ovarian serous neoplasms (low-grade serous carcinoma and serous borderline tumor) associated with high-grade serous carcinoma or undifferentiated carcinoma: report of a series of cases of an unusual phenomenon. Am J Surg Pathol 2012; 36, 368–75. [PubMed: 22082603]

[17]. Nik NN, Vang R, Shih Ie M, et al. Origin and pathogenesis of pelvic (ovarian, tubal, and primary peritoneal) serous carcinoma. Annu Rev Pathol 2014; 9, 27–45. [PubMed: 23937438]

[18]. Kurman RJ and Shih Ie M. Molecular pathogenesis and extraovarian origin of epithelial ovarian cancer--shifting the paradigm. Hum Pathol 2011; 42, 918–31. [PubMed: 21683865]

[19]. Verhaak RG, Tamayo P, Yang JY, et al. Prognostically relevant gene signatures of high-grade serous ovarian carcinoma. J Clin Invest 2013; 123, 517–25. [PubMed: 23257362]

[20]. Tothill RW, Tinker AV, George J, et al. Novel molecular subtypes of serous and endometrioid ovarian cancer linked to clinical outcome. Clin Cancer Res 2008; 14, 5198–208. [PubMed: 18698038]

[21]. Lee PS, Buchan AM, Hsueh AJ, et al. Intracellular calcium mobilization in response to the activation of human wild-type and chimeric gonadotropin receptors. Endocrinology 2002; 143, 1732–40. [PubMed: 11956155]

[22]. Lv X, He C, Huang C, et al. Timely expression and activation of YAP1 in granulosa cells is essential for ovarian follicle development. FASEB J 2019; 33, 10049–10064. [PubMed: 31199671]

[23]. Wang C, Lv X, Jiang C, et al. Transforming growth factor alpha (TGFalpha) regulates granulosa cell tumor (GCT) cell proliferation and migration through activation of multiple pathways. PLoS One 2012; 7, e48299. [PubMed: 23155381]

[24]. Fu D, Lv X, Hua G, et al. YAP regulates cell proliferation, migration, and steroidogenesis in adult granulosa cell tumors. Endocr Relat Cancer 2014; 21, 297–310. [PubMed: 24389730]

[25]. Wang C, Lv X, He C, et al. The G-protein-coupled estrogen receptor agonist G-1 suppresses proliferation of ovarian cancer cells by blocking tubulin polymerization. Cell Death Dis 2013; 4, e869. [PubMed: 24136233]

[26]. Lv X, He C, Huang C, et al. G-1 Inhibits Breast Cancer Cell Growth via Targeting Colchicine-Binding Site of Tubulin to Interfere with Microtubule Assembly. Mol Cancer Ther 2017; 16, 1080–1091. [PubMed: 28258163]

[27]. He C, Mao D, Hua G, et al. The Hippo/YAP pathway interacts with EGFR signaling and HPV oncoproteins to regulate cervical cancer progression. EMBO Mol Med 2015; 7, 1426–49. [PubMed: 26417066]

[28]. Hua G, He C, Lv X, et al. The four and a half LIM domains 2 (FHL2) regulates ovarian granulosa cell tumor progression via controlling AKT1 transcription. Cell Death Dis 2016; 7, e2297. [PubMed: 27415427]

[29]. Wang C, Lv X, Jiang C, et al. The putative G-protein coupled estrogen receptor agonist G-1 suppresses proliferation of ovarian and breast cancer cells in a GPER-independent manner. Am J Transl Res 2012; 4, 390–402. [PubMed: 23145207]

[30]. Dong J, Feldmann G, Huang J, et al. Elucidation of a universal size-control mechanism in Drosophila and mammals. Cell 2007; 130, 1120–33. [PubMed: 17889654]

[31]. Zhao B, Wei X, Li W, et al. Inactivation of YAP oncoprotein by the Hippo pathway is involved in cell contact inhibition and tissue growth control. Genes Dev 2007; 21, 2747–61. [PubMed: 17974916]

[32]. Pan D The hippo signaling pathway in development and cancer. Dev Cell 2010; 19, 491–505. [PubMed: 20951342]

[33]. Reddy BV and Irvine KD. Regulation of Hippo signaling by EGFR-MAPK signaling through Ajuba family proteins. Dev Cell 2013; 24, 459–71. [PubMed: 23484853]

[34]. Shamir ER and Ewald AJ. Three-dimensional organotypic culture: experimental models of mammalian biology and disease. Nat Rev Mol Cell Biol 2014; 15, 647–64. [PubMed: 25237826]

[35]. Hsueh AJ, Kawamura K, Cheng Y, et al. Intraovarian control of early folliculogenesis. Endocr Rev 2014, er20141020.

[36]. Liu-Chittenden Y, Huang B, Shim JS, et al. Genetic and pharmacological disruption of the TEAD-YAP complex suppresses the oncogenic activity of YAP. Genes Dev 2012; 26, 1300–5. [PubMed: 22677547]

[37]. Nishi Y, Yanase T, Mu Y, et al. Establishment and characterization of a steroidogenic human granulosa-like tumor cell line, KGN, that expresses functional follicle-stimulating hormone receptor. Endocrinology 2001; 142, 437–45. [PubMed: 11145608]

[38]. Bao B and Garverick HA. Expression of steroidogenic enzyme and gonadotropin receptor genes in bovine follicles during ovarian follicular waves: a review. J Anim Sci 1998; 76, 1903–21. [PubMed: 9690647]

[39]. Hsueh AJ, Jones PB, Adashi EY, et al. Intraovarian mechanisms in the hormonal control of granulosa cell differentiation in rats. J Reprod Fertil 1983; 69, 325–42. [PubMed: 6350574]

[40]. Richards JS, Fitzpatrick SL, Clemens JW, et al. Ovarian cell differentiation: a cascade of multiple hormones, cellular signals, and regulated genes. Recent Prog Horm Res 1995; 50, 223–54. [PubMed: 7740159]

[41]. Hunzicker-Dunn M and Maizels ET. FSH signaling pathways in immature granulosa cells that regulate target gene expression: branching out from protein kinase A. Cell Signal 2006; 18, 1351–9. [PubMed: 16616457]

[42]. Hillier SG Gonadotropic control of ovarian follicular growth and development. Mol Cell Endocrinol 2001; 179, 39–46. [PubMed: 11420129]

[43]. Li R, Liang J, Ni S, et al. A mesenchymal-to-epithelial transition initiates and is required for the nuclear reprogramming of mouse fibroblasts. Cell Stem Cell 2010; 7, 51–63. [PubMed: 20621050]

[44]. Samavarchi-Tehrani P, Golipour A, David L, et al. Functional genomics reveals a BMP-driven mesenchymal-to-epithelial transition in the initiation of somatic cell reprogramming. Cell Stem Cell 2010; 7, 64–77. [PubMed: 20621051]

[45]. Bayasula A Iwase T. Kiyono, et al. Establishment of a human nonluteinized granulosa cell line that transitions from the gonadotropin-independent to the gonadotropin-dependent status. Endocrinology 2012; 153, 2851–60. [PubMed: 22467494]

[46]. Rainey WH, Sawetawan C, Shay JW, et al. Transformation of human granulosa cells with the E6 and E7 regions of human papillomavirus. J Clin Endocrinol Metab 1994; 78, 705–10. [PubMed: 8126145]

[47]. Bowtell DD, Bohm S, Ahmed AA, et al. Rethinking ovarian cancer II: reducing mortality from high-grade serous ovarian cancer. Nat Rev Cancer 2015; 15, 668–79. [PubMed: 26493647]

[48]. Zhao T and Xu Y. p53 and stem cells: new developments and new concerns. Trends Cell Biol 2010; 20, 170–5. [PubMed: 20061153]

[49]. Yi L, Lu C, Hu W, et al. Multiple roles of p53-related pathways in somatic cell reprogramming and stem cell differentiation. Cancer Res 2012; 72, 5635–45. [PubMed: 22964580]

[50]. Bonizzi G, Cicalese A, Insinga A, et al. The emerging role of p53 in stem cells. Trends Mol Med 2012; 18, 6–12. [PubMed: 21907001]

[51]. Dittmer D, Pati S, Zambetti G, et al. Gain of function mutations in p53. Nat Genet 1993; 4, 42–6. [PubMed: 8099841]

[52]. Oren M and Rotter V. Mutant p53 gain-of-function in cancer. Cold Spring Harb Perspect Biol 2010; 2, a001107. [PubMed: 20182618]

[53]. Muller PA and Vousden KH. p53 mutations in cancer. Nat Cell Biol 2013; 15, 2–8. [PubMed: 23263379]

[54]. Halder G and Johnson RL. Hippo signaling: growth control and beyond. Development 2011; 138, 9–22. [PubMed: 21138973]

[55]. Zhao B, Lei QY, and Guan KL. The Hippo-YAP pathway: new connections between regulation of organ size and cancer. Curr Opin Cell Biol 2008; 20, 638–46. [PubMed: 18955139]

[56]. Barry ER and Camargo FD. The Hippo superhighway: signaling crossroads converging on the Hippo/Yap pathway in stem cells and development. Curr Opin Cell Biol 2013; 25, 247–53. [PubMed: 23312716]

[57]. Zeng Q and Hong W. The emerging role of the hippo pathway in cell contact inhibition, organ size control, and cancer development in mammals. Cancer Cell 2008; 13, 188–92. [PubMed: 18328423]

[58]. Harvey KF, Zhang X, and Thomas DM. The Hippo pathway and human cancer. Nat Rev Cancer 2013; 13, 246–57. [PubMed: 23467301]

[59]. Moroishi T, Hansen CG, and Guan KL. The emerging roles of YAP and TAZ in cancer. Nat Rev Cancer 2015; 15, 73–9. [PubMed: 25592648]

[60]. Yu FX, Zhao B, and Guan KL. Hippo Pathway in Organ Size Control, Tissue Homeostasis, and Cancer. Cell 2015; 163, 811–28.

[61]. Hua G, Lv X, He C, et al. YAP induces high-grade serous carcinoma in fallopian tube secretory epithelial cells. Oncogene 2016; 35, 2247–65. [PubMed: 26364602]

[62]. Lian I, Kim J, Okazawa H, et al. The role of YAP transcription coactivator in regulating stem cell self-renewal and differentiation. Genes Dev 2010; 24, 1106–18. [PubMed: 20516196]

[63]. Musah S, Wrighton PJ, Zaltsman Y, et al. Substratum-induced differentiation of human pluripotent stem cells reveals the coactivator YAP is a potent regulator of neuronal specification. Proc Natl Acad Sci U S A 2014; 111, 13805–10. [PubMed: 25201954]

[64]. Ramos A and Camargo FD. The Hippo signaling pathway and stem cell biology. Trends Cell Biol 2012; 22, 339–46. [PubMed: 22658639]

[65]. Mo JS, Park HW, and Guan KL. The Hippo signaling pathway in stem cell biology and cancer. EMBO Rep 2014; 15, 642–56. [PubMed: 24825474]

[66]. Panciera T, Azzolin L, Fujimura A, et al. Induction of Expandable Tissue-Specific Stem/Progenitor Cells through Transient Expression of YAP/TAZ. Cell Stem Cell 2016; 19, 725–737. [PubMed: 27641305]

[67]. Flesken-Nikitin A, Hwang CI, Cheng CY, et al. Ovarian surface epithelium at the junction area contains a cancer-prone stem cell niche. Nature 2013; 495, 241–5. [PubMed: 23467088]

[68]. Ng A, Tan S, Singh G, et al. Lgr5 marks stem/progenitor cells in ovary and tubal epithelia. Nat Cell Biol 2014; 16, 745–57. [PubMed: 24997521]

[69]. Rastetter RH, Bernard P, Palmer JS, et al. Marker genes identify three somatic cell types in the fetal mouse ovary. Dev Biol 2014; 394, 242–52. [PubMed: 25158167]

[70]. Dzafic E, Stimpfel M, and Virant-Klun I. Plasticity of granulosa cells: on the crossroad of stemness and transdifferentiation potential. J Assist Reprod Genet 2013; 30, 1255–61. [PubMed: 23893266]

[71]. Varras M, Griva T, Kalles V, et al. Markers of stem cells in human ovarian granulosa cells: is there a clinical significance in ART? J Ovarian Res 2012; 5, 36. [PubMed: 23164047]

[72]. Kossowska-Tomaszczuk K and De Geyter C. Cells with stem cell characteristics in somatic compartments of the ovary. Biomed Res Int 2013; 2013, 310859. [PubMed: 23484108]

[73]. O'Connor MJ Targeting the DNA Damage Response in Cancer. Mol Cell 2015; 60, 547–60. [PubMed: 26590714]

[74]. Deng CX BRCA1: cell cycle checkpoint, genetic instability, DNA damage response and cancer evolution. Nucleic Acids Res 2006; 34, 1416–26. [PubMed: 16522651]

[75]. Jopling C, Boue S, and Izpisua Belmonte JC. Dedifferentiation, transdifferentiation and reprogramming: three routes to regeneration. Nat Rev Mol Cell Biol 2011; 12, 79–89. [PubMed: 21252997]

[76]. Friedmann-Morvinski D and Verma IM. Dedifferentiation and reprogramming: origins of cancer stem cells. EMBO Rep 2014; 15, 244–53. [PubMed: 24531722]

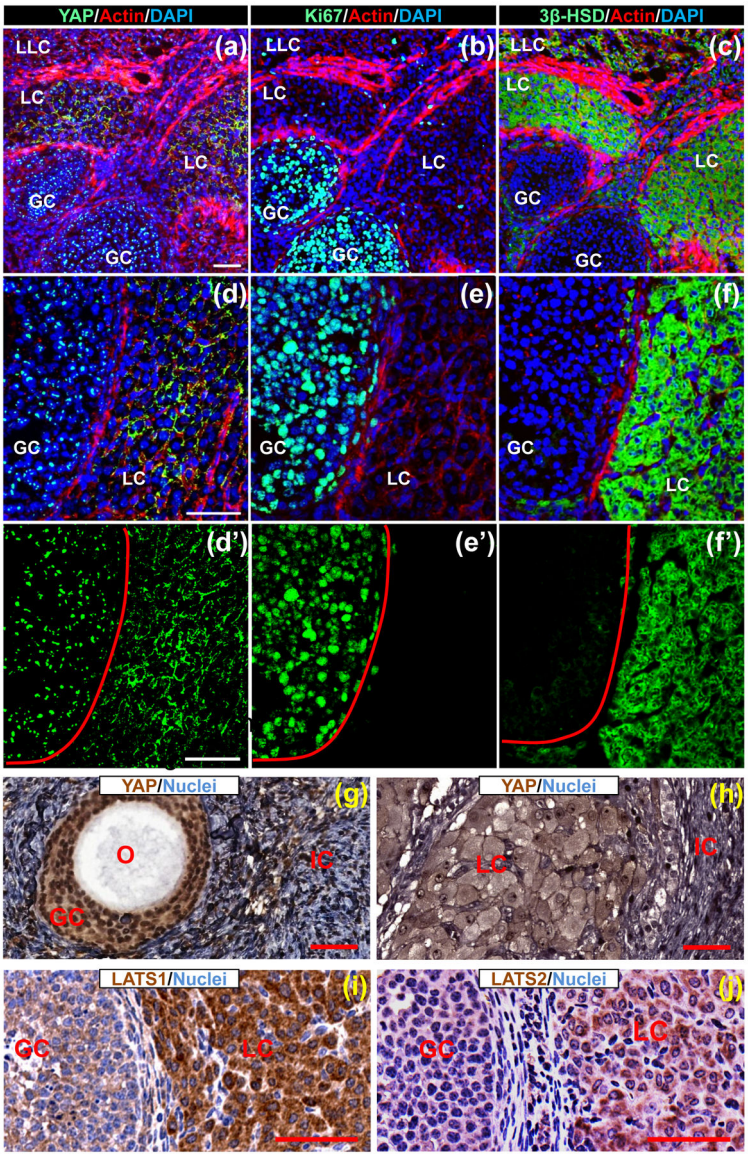

Figure 1. Differential expression of YAP1 protein in the proliferative and differentiated granulosa cells of mouse and human ovaries.

(a)-(c): Expression of YAP1 (a), Ki-67 (b), and 3β-HSD (c) in the mouse ovary. Proteins were determined in serial frozen sections using fluorescent immunohistochemistry. Target proteins were visualized using Alexa-488 (green). Actin was visualized by rhodamine-phalloidin (red). Nuclei were stained by DAPI (blue). Scale bar: 50μm. **(d)-(f)** High-resolution images showing expression of YAP1 (d), Ki-67 (e), and 3β-HSD (f) in the mouse ovary. Please note the expression of nuclear YAP1 in proliferative granulosa cells (GCs) in growing follicles and cytoplasmic expression of YAP1 in terminally differentiated granulosa cells (LC) in the corpus luteum. Scale bar: 50μm. **(d')-(f')** Single channel (green) images showing the immunosignal localization of YAP1 (predominantly localized to nuclei of GCs in the growing follicle and cytoplasm of luteinized GCs in corpus luteum), Ki-67 (nuclei of proliferative GCs in growing follicles) and 3β-HSD (cytoplasm of terminally differentiated GCs in corpus luteum) in (d), (e) and (f), respectively. **(g)-(h)**

Representative images showing the expression of YAP1 in the GCs of a growing follicle and in terminally differentiated granulosa cells (LC) in a corpus luteum of human ovaries. O: oocyte; IC: interstitial cells. Scale bar: 50 μm. **(i)-(j)** expression of LATS1 and LATS2, the upstream suppressor of YAP1, in proliferative GCs of growing follicles and luteal cells (LC, terminally differentiated granulosa cells) of mouse ovarian follicles detected by IHC. Scale bar: 50 μm.

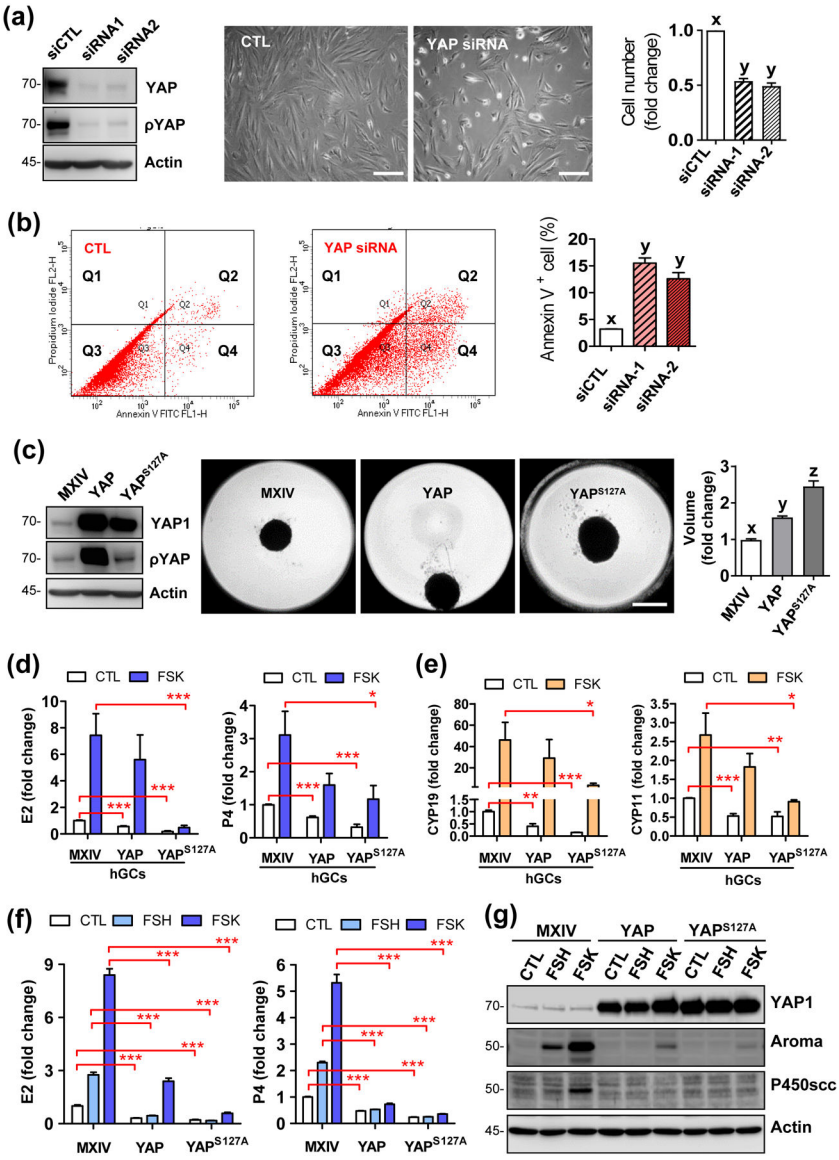

Figure 2. YAP1 promotes proliferation, supports survival, but blocked gonadotropin-induced steroidogenesis of hGCs.

(a) Left panel: Western blot showing high efficiency of YAP1 knockdown with YAP1-targeting siRNA1 and siRNA2. Non-targeting siRNA was used as control (siCTL); middle panel: representative pictures show morphological changes of cultured hGCs incubated in the growing medium for 5 days after knocking down of YAP1 protein, Scale bar: 200 μm; right panel: bar graph showing cell number change of hGCs incubated in growing medium for 5 days after knockdown of YAP1 protein. Each bar represents the mean ± SEM (n = 4). Bars with different letters are significantly different from each other ($P < 0.01$). **(b)** Representative images showing changes in cell death rate in hGCs with or without (CTL) knockdown of YAP1 proteins. Cell death was determined with an Annexin V-FITC/PI staining kit and sorted by flow cytometry. Right bar graph showing the Annexin V positive hGCs with or without YAP1 knockdown. Each bar represents the mean ± SEM ($n = 3$). Bars with different letters are significantly different from each other ($P < 0.01$).

(c) Left panel: western blot showing YAP1 and phosphorylated YAP1 (Ser127) expressions in hGC-MXIV, hGC-YAP, and hGC-YAP^{S127A} cells. β-Actin was used as loading control; middle panel: Representative images showing the spheroids from hGC-MXIV, hGC-YAP, and hGC-YAP^{S127A} cells incubated in a 3D-hanging drop culture system for 5 days, Scale bar: 500 μm; Right panel: Bar graph showing volumes of the spheroids from these cells. Each bar represents the mean ± SEM (n = 6). Bars with different letters are significantly different from each other (P < 0.01). **(d)** Hyperactivation of YAP1 compromised basal (CTL) and FSK-induced production of estrogen and progesterone in the primary culture of hGCs. Each bar represents the mean ± SEM ($n \geq 5$). *: P < 0.05; ***: P < 0.001. FSK: forskolin (10 μmol/L). **(e)** Hyperactivation of YAP1 decreased basal (CTL) and FSK-induced transcription of CYP19A1 and CYP11A1 genes in the primary culture of human granulosa cells. Each bar represents the mean ± SEM ($n \geq 5$). *: P < 0.05; ***: P < 0.001. **(f)** Hyperactivation of YAP1 reduced basal and FSH- and FSK-induced production of estrogen and progesterone in KGN cells. Each bar represents the mean ± SEM ($n \geq 4$). ***: P < 0.001. **(g)** Western blot results showing that hyperactivation of YAP1 compromised FSH- and FSK-induced expression of key enzymes for steroidogenesis in KGN cells. Aroma: aromatase; P450SCC: P450 side-chain cleavage enzyme. β-Actin was used as a protein loading control.

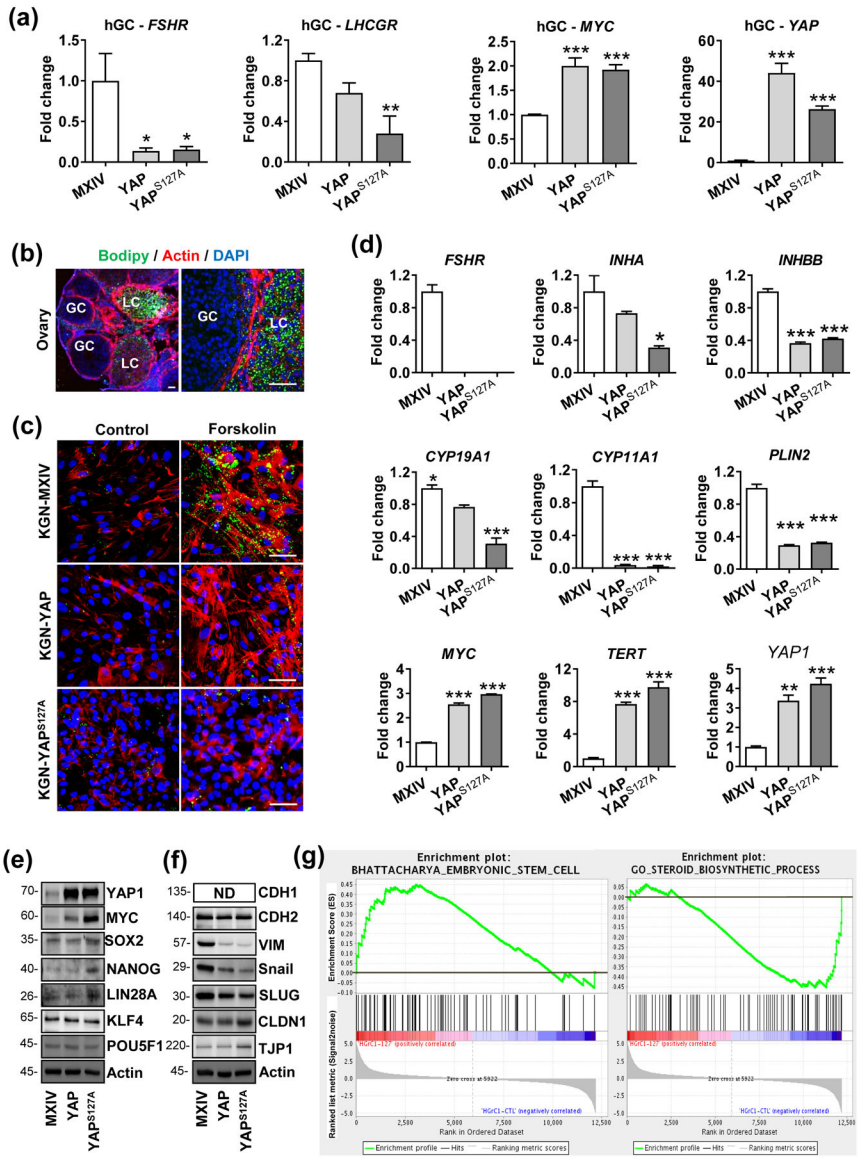

Figure 3. Ectopic expression of YAP1 induced dedifferentiation and reprogramming of hGCs.

(a) Ectopic expression of YAP1 suppressed expression of granulosa cell differentiation-associated key genes (*FSHR* and *LHCGR*) and increased expression of cell reprogramming factor (*MYC*) in primary culture of ovarian granulosa cells. Each bar represents the mean ± SEM (n ≥ 3). *: $P < 0.05$, **: $P < 0.01$, ***: $P < 0.001$, compared with control. **(b)** Representative images showing lipid droplets stained with BODIPY in the ovarian tissues. Please note the negative staining in the proliferative granulosa cells (GC) and strong positive staining in the terminally differentiated granulosa cells (LC). **(c)** Representative images showing lipid drops stained with BODIPY in the KGN-MX, KGN-YAP, and KGN-YAP^{S127A} cells treated with or without forskolin (FSK) for 3 days. Please note the positive staining in forskolin-induced KGN-MX control cells and the negative staining in YAP1 and YAP^{S127A} cells. Scale Bar: 50 μm. **(d)** Expression of key molecules of cell differentiation (*FSHR, INHA, INHBB, CYP19A1, CYP11A1,* and *PLIN2*), and cellular reprogramming

factors (*MYC* and *TERT*) in KGN cells with or without YAP1 overexpression. Each bar represents the mean ± SEM (n ≥ 3). *: $P < 0.05$, **: $P < 0.01$, ***: $P < 0.001$, compared with control. **(e)** Expression of cell-reprogramming factors detected by western blots in KGN cells with or without ectopic YAP1 expression. β-Actin was used as the loading control. All experiments are repeated at least three times, and the representative blots were presented. **(f)** Western blots showing expression of proteins associated with the mesenchymal–epithelial transition (MET) after YAP1 overexpression in KGN cells. β-Actin was used as a loading control. All experiments are repeated at least three times, and the representative blots were presented. **(g)** YAP1 induced enrichment of genes associated with cellular reprogramming and stemness in HGrC1 cells. GSEA was performed based on the gene expression profiling on HGrC1-MX (HGrC1-CTL, n=3) and HGrC1-YAP^{S127A} cells (n=3) using RNA-seq analysis. Left panel: Enrichment of genes-associated with embryonic stem cells from the BHATTACHARYA_EMBRYONIC_STEM_CELL gene sets. Right panel: Enrichment of genes-associated with granulosa cell differentiation from the GO_STEROID- BIOSYNTHETIC_PROCESS gene sets.

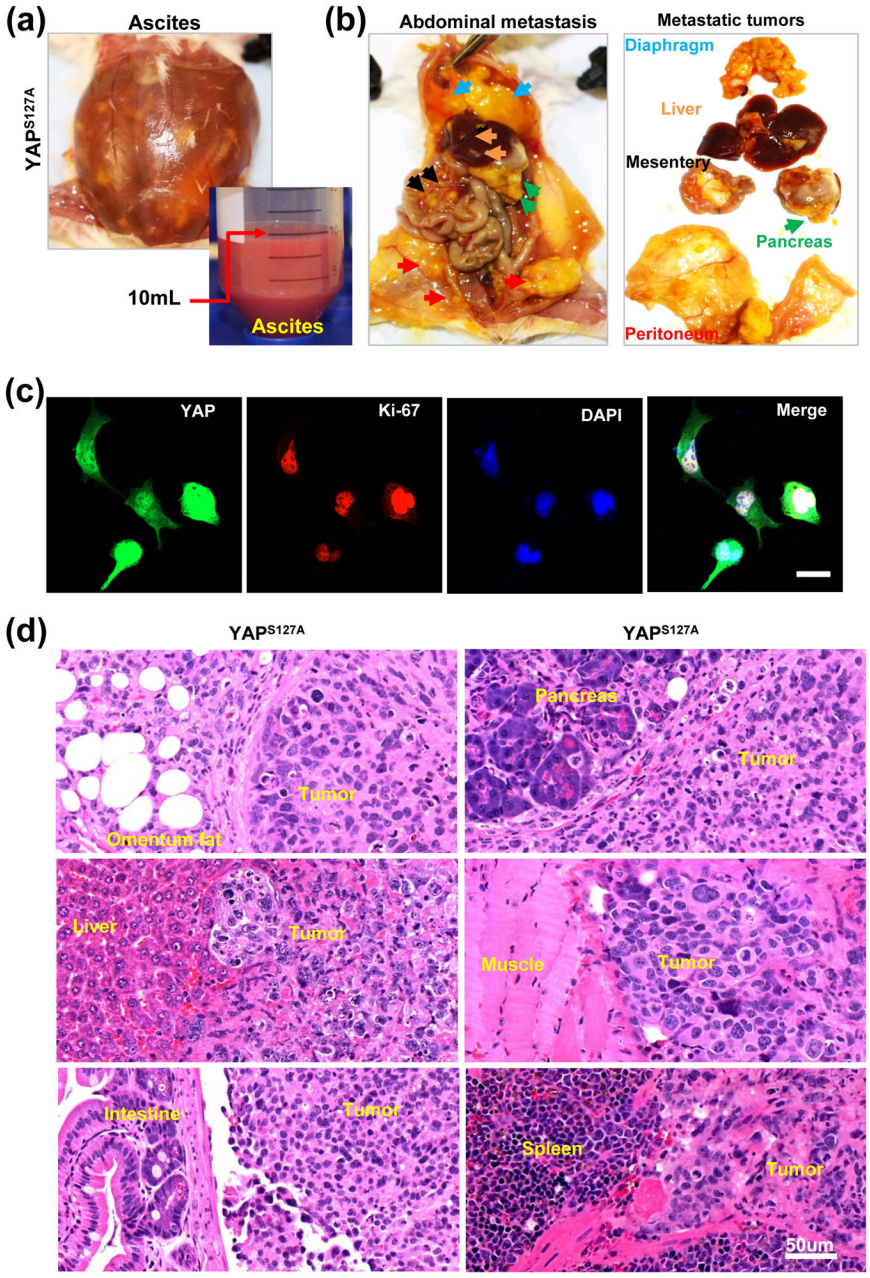

Figure 4. YAP1 induces metastatic cancer from less-differentiated granulosa cells.

(a) - (b) Representative images showing the malignant ovarian cancers derived from HGrC1-YAP^{S127A} cells. Representative images in (a) showing accumulation of a large amount of ascites in the abdomen of tumor carrying mice; representative images in (b) showing metastatic spread of granulosa cell-derived cancers in the mouse abdomen organs and tissues, including peritoneum (red arrowhead), mesentery (black arrowhead), diaphragm (blue arrowhead), pancreas (green arrowhead), and liver (orange arrowhead). **(c)** Fluorescent immunohistochemistry showing expression of YAP1 (in green) and Ki67 (in red) proteins in malignant cancer cells separated from mouse ascites. Nuclei were stained with DAPI

(blue). Scale bar: 20 μm. **(d)** Representative images showing the histology of the metastatic malignant ovarian cancer derived from HGrC1-YAP^{S127A} cells. Scale bar: 50 μm.

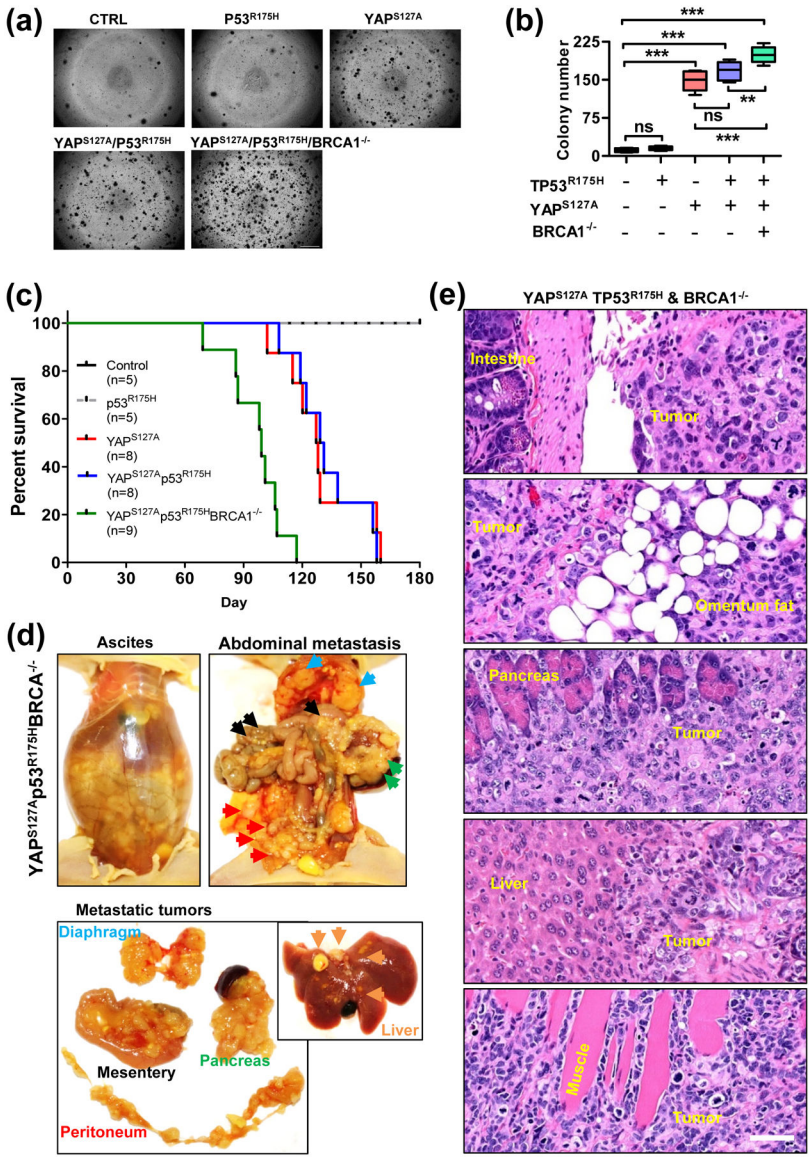

Figure 5. Histopathological features of YAP1-induced metastatic cancer from less-differentiated granulosa cells.

(a) Representative images showing colonies formed by HGrC1-CTL, HGrC1-TP53^{R175H}, HGrC1-YAP^{S127A}, HGrC1-YAP^{S127A}/TP53^{R175H}, and HGrC1-YAP^{S127A}/TP53^{R175H}/BRCA1$^{-/-}$ cells. Scale bar: 500 μm. **(b)** Quantitative data showing colonies derived from each type of cells in (A). Each bar represents the mean ± SEM (n ≥ 6). **: p <0.01, ***: p < 0.001. **(c)** Kaplan-Meier Survival plot showing the survival rate of immunodeficient mice implanted with HGrC1-CTL cells (n = 5, black curve), HGrC1-TP53^{R175H} cells (n = 5, grey curve), HGrC1-YAP^{S127A} cells (n = 8, red curve), HGrC1-YAP^{S127A}/TP53^{R175H} cells (n=8, blue curve), and HGrC1-YAP^{S127A}/TP53^{R175H}/BRCA1$^{-/-}$ cells (n = 9, green curve). **(d)** Representative images showing the malignant ovarian cancers derived from HGrC1-YAP^{S127A}/TP53^{R175H}/BRCA1$^{-/-}$ cells. Top left panel: representative images showing accumulation of a large amount of ascites in the abdomen of tumor carrying mice; Representative images in the top right and lower panels showing the metastatic spread

of granulosa cell-derived cancers in the mouse abdomen organs and tissues, including peritoneum (red arrowhead), mesentery (black arrowhead), diaphragm (blue arrowhead), pancreas (green arrowhead), and liver (orange arrowhead). **(e)** Representative images showing the histology of the metastatic malignant ovarian cancer derived from YAP^{S127A}/$TP53^{R175H}$/$BRCA1^{-/-}$ cells. Scale bar: 50 μm.

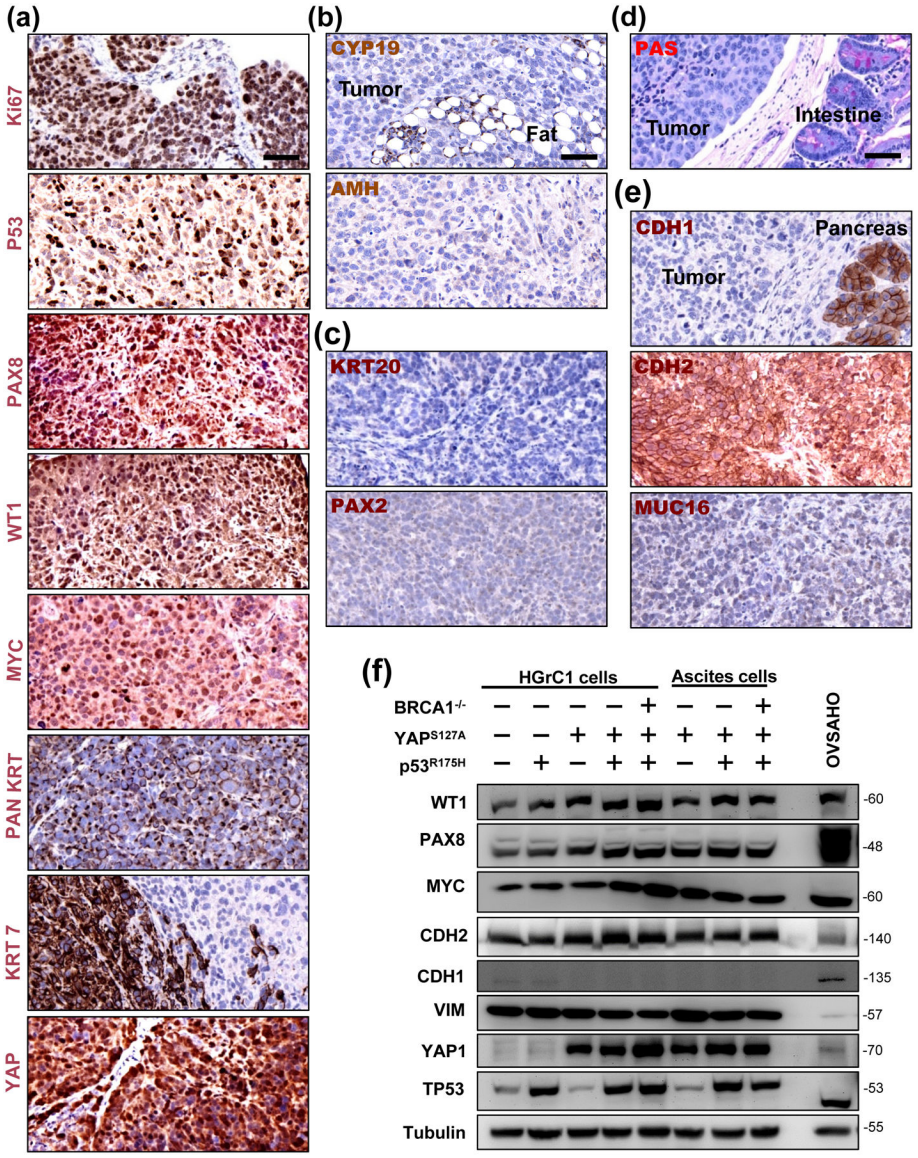

Figure 6. YAP1 induced High grade ovarian cancers with serous features from less-differentiated granulosa cells.

(a) Molecular features of tumors derived from the xenograft mouse model of YAP^{S127A}/$TP53^{R175H}$/$BRCA1^{-/-}$ cells. Representative image showing high level expression of Ki-67, nuclear TP53, PAN keratin (PAN KRT), Keratin 7 (KRT7), PAX8, WT-1, MYC, and YAP1 protein in tumor tissues analyzed by immunohistochemistry. Scale bar: 50 μm. **(b)** Representative images showing that tumor tissues are negative for the expression of granulosa cell tumor markers (CYP19A1 and AMH). **(c)** Representative images showing that tumor tissues are negative for low grade serous carcinoma and mucinous ovarian cancer markers (PAX2 and KRT20). **(d)** Representative images showing that tumor tissues are negative for mucinous cancer markers (PAS staining). **(e)** Representative images showing that tumor tissues have high expression of CDH2 (N-cadherin), but low expression of CDH1 (E-cadherin) and MUC16 (CA125), which is a molecular feature of the recently identified mesenchymal type of ovarian high grade serous cancer. Scale

bar: 50 μm. **(f)** Representative blots showing expression of WT1, PAX8, MYC, CDH2 (N-cadherin), CDH1 (E-cadherin), VIM (vimentin), TP53, and in established HGrC1-CTL cells, HGrC1- $TP53^{R175H}$ cells, HGrC1-YAP^{S127A} cells, HGrC1-YAP^{S127A}/$TP53^{R175H}$ cells, and HGrC1-YAP^{S127A}/$TP53^{R175H}$/$BRCA1^{-/-}$ cells. Expressions of these biomarkers were also examined in ascites tumor cells collected from immunodeficient mice carrying tumors from HGrC1-YAP^{S127A}, HGrC1-YAP^{S127A}/$TP53^{R175H}$, and HGrC1-YAP^{S127A}/$TP53^{R175H}$/$BRCA1^{-/-}$ cells. OVSAHO cells were used as control.

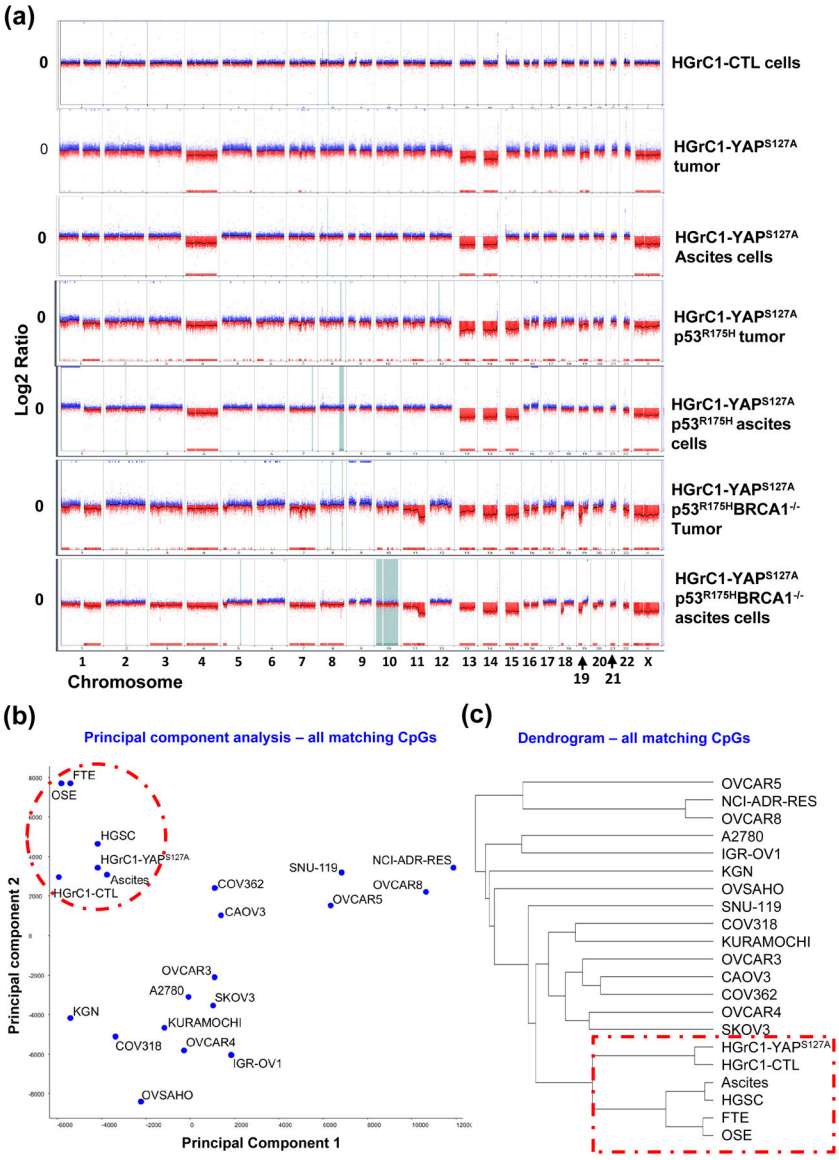

Figure 7. Genomic and epigenomic evidence that metastatic cancers derived from less-differentiated granulosa cells resemble ovarian HGSCs.

(a) Tumors and ascites cells exhibited severe genomic instability as in human ovarian HGSC. aCGH analysis results showing DNA copy number changes of tumor tissues and ascites cells, as well as control cells. The Y-axis represents gain (positive) or loss (negative) of copy number, while the X-axis represents each chromosome. CTL: HGrC1-CTL cells; HGrC1-YAP^{S127A} tumor & HGrC1-YAP^{S127A} ascites: tumor tissue and ascites cells that were harvested from mouse implanted with HGrC1-YAP^{S127A} cells; HGrC1-YAP^{S127A}/TP53^{R175H} tumor & HGrC1-YAP^{S127A}/TP53^{R175H} ascites: tumor tissue and ascites cells that were harvested from mouse implanted with HGrC1-YAP^{S127A}/TP53^{R175H} cells; YAP^{S127A}/TP53^{R175H}/BRCA1$^{-/-}$ tumor & YAP^{S127A}/TP53^{R175H}/BRCA1$^{-/-}$ ascites: tumor tissue and ascites cells that were harvested from mouse implanted with HGrC1-YAP^{S127A}/TP53^{R175H}/BRCA1$^{-/-}$ cells. **(b)** Principle component analysis based on the genome-wide DNA methylation CpG profile. Note that fallopian tube epithelial cells (FTE), OSE cells,

HGrC1, and HGrC1-YAP^{S127A} cells are grouped with ovaria HGSC and ascites cells from ovarian HGSC. **(c)** Dendrogram classification analysis based on the genome-wide DNA CpG methylation profile. Note that FTE cells, OSE cells, HGrC1, and HGrC1-YAP^{S127A} cells have the closest relationship with ovarian HGSCs.